Civil and Environmental Science Journal
Vol. 5, No. 1, pp. 026-044, 2022

Analysis of Changes in Land Use Patterns for Erosion and Sediment Prediction

Syamsul Arifin[1,2,*], Ery Suhartanto[2], Ussy Andawayanti[2]

[1] Hydrology Departement, PT. Globetek Glory Konsultan, Manado, 95125, Indonesia
[2] Water Resources Engineering Department, Universitas Brawijaya, Malang, 65145, Indonesia

*techoest.1980@gmail.com

Received 12-01-2022; accepted 05-03-2022

Abstract. The Amprong watershed has an area of ± 252.94 km². The increasing population causes the demand for land to increase. GIS analyzes changes with the factors of change that occur. The purpose of the study was to determine the pattern of land-use change in the Amprong watershed on erosion and sedimentation. Idrisi Selva for use change analysis and SWAT for erosion and sediment. From the results of land cover modeling, it can be seen that the trend of forest land cover change from 2008, 2013, and 2018 continued to decline with an average of 11.69% of land cover in 2008. In contrast to settlements, it always increased by an average of 9.29%. Meanwhile, land cover changes in 2018 and 2028 decreased by 21.40%, plantations decreased by 4.33%, open land decreased by 42.11%, settlements increased by 46.47%, rice fields increased by 0.60%, and shrubs increased by 4.63%. The Kappa Index of Agreement validation shows a K standard value of 0.85 which means that the modeling is scientifically accepted. The results of hydrological modeling in 2018 were 1,021,237.49 tons/ha/year, erosion was 752,973.95 tons/ha/year and in 2028 it was 1,886,689.64 tons/ha/year, erosion was 1,069,631.09 tons/year.

Keywords: Amprong Watershed, Arcswat 2012, Erosion, Idrisi Selva, Sedimentation

1. Introduction

The Amprong River is one of the tributaries of the Brantas River, with an area of ± 252.94 km². The Amprong watershed is located in Malang Regency and Malang City [1]. The population growth rate in Malang Regency and Malang City which continues to increase for the average population growth rate of Malang Regency based on data from the Central Statistics Agency of Malang Regency is 0.86% per year, while for the population growth rate of Malang City based on the Central Statistics Agency Malang City is 0.70% per year [2].

Kedung Kandang weir or residents call it Rolak Kedung Kandang, whose existence is vital for irrigation in the Kedung Kandang Irrigation Area, is the main structure in the Kedung Kandang Irrigation Area which has an area of 5160 Ha that covers the area of Malang City and Malang Regency. Kedung

Cite this as: Arifin, S., Ery, S., & Andawayanti, U. (2022). Analysis of Changes in Land Use Patterns for Erosion and Sediment Prediction. Civil and Environmental Science Journal (Civense), 5(1), 26-44. doi: https://doi.org/10.21776/ub.civense.2022.00501.4

Kandang Dam coordinates 7°59'22.25" South Latitude and 112°39'11.28" East Longitude or downstream of the Amprong Watershed. Weir is the main structure that functions to raise the water level to flow into the intake of the irrigation network of Kedung Kandang. The Kedung Kandang intake is at ± 600 m upstream of the weir. The water comes from the Amprong River and the Kalisari Suppletion Channel [3]. Due to high erosion resulting in sedimentation upstream of the Kedung Kandang weir. In the dry season, the water discharge in the Amprong River has decreased, impacting the level of adequacy of irrigation water needs in the Kedung Kandang Irrigation Area and the smooth production of sugar at the Krebet Sugar Factory. These conditions can be overcome by the existence of the Kalisari Suppletion Channel due to the high sediment upstream of the Kedung Kandang Weir, causing the water discharge from the Kalisari Suppletion Channel to be wasted through the weir spillway [4], [5].

Changes in land cover can be analyzed by using remote sensing and Geographic Information Systems, namely satellite images. Analysis of change and modelling for land cover prediction in a watershed can be done with the assist of Idrisi Selva software [6], [7].

While the easiest analysis to describe complex watershed conditions is to model it. The watershed hydrological model describes the interactions between variables in the watershed context. The development of the watershed hydrological model is in line with the development of Geographic Information System (GIS) and remote sensing technology [8]. The Watershed hydrological model cover that is often used is spatial modelling based on land cover data, forecasting and predicting the condition of a change for flood, drought, erosion, sedimentation, and other conditions [2]. The Soil and Water Assessment Tool (SWAT) is a hydrological model developed to predict the effects of land management on the result of water, sediments, pesticide loads, and agricultural chemicals [9]–[11].

The problems that occur are caused by changes in land cover that are not well planned. Therefore, there is a need for research on the impact of land-use changes on the level of erosion that causes sedimentation downstream of the Amprong watershed. In the end, to obtain the right handling solution to maintain the availability of irrigation water needs in the Kedung Kandang Irrigation Area and obtain a basis for determining the watershed management in the future [5]. Therefore, the purpose of the study was to assess the pattern of land-use change in the Amprong watershed on erosion and sedimentation

2. Data and Method

2.1 Data

The data needed for this analysis, namely Earth Map Scale 1: 25,000, DEM Map, Soil Type Data, Rain Station Coordinate Data, Daily rainfall data from the nearest rain station in the Amprong watershed for 10 years (2008-2017), Discharge measurement data, Temperature data, Solar radiation data, Relative humidity data, Wind speed/velocity data, Landsat 7 ETM imagery dated June 20th, 2008, Landsat 8 OLI/TIRS imagery dated August 13th, 2013 and July 26th, 2018.

2.2 Method

2.2.1. Rain Data Statistical Test

Consistency Test

The data consistency test was carried out to find out whether there were data deviations in the available rain data so that it could be seen whether the data was suitable to be used in the subsequent hydrological analysis or not. The double mass curve method was used [12].

Homogeneity Test

A series of hydrological data presented chronologically as a function of the same time is called a periodic series. Field data published generally are discharge data, rainfall data, and others. The data is arranged in the form of a periodic series, so it must be tested before being used for further analysis. The data testing intended are: (1) No Trend Test; (2) Stationary Test; (3) Persistency Test. The three stages of testing are often referred to as data filtering (data screening) [13].

2.2.2 Regional Average Rainfall

The rainfall data for the rain station post will be used in the form of regional average rainfall data calculated using the Thiessen Polygon Method [6], [14].

2.2.3 Land use change analysis

The basic map that needs to be prepared is the earth map. The Landsat 7 ETM satellite imagery layout in 2008 and Landsat 8 OLI/TIRS in 2013 and 2018 for the Kali Amprong Watershed projected to the 49s UTM (*Universal Transverse Mercator*) Zone. The map of the earth is used to obtain spatial administrative analysis data sourced from the Geospatial Information Agency/Badan Informasi Geospatial (BIG), Digital Elevation Model (DEM) data, which is obtained from DEMNAS data downloaded from https://tanahair.indonesia.go.id.

Basic image management includes geometric and radiometric corrections and gap filling for the 2008 image because there was a gap fill due to the sensor SLC off on the Landsat 7 ETM device in 2008. Gap filling process using ENVI 5 software. Remote sensing data is in the form of digital data. The use of the data requires special hardware and software for processing. Analysis and interpretation can be conducted in two ways:

a. Digital processing and analysis
b. Visual analysis and interpretation.

Both of these methods have advantages and disadvantages. At least both methods are used together to complement each other. Digital processing functions to read data, display data, modify and process, extract data automatically, store, design map formats, and print. Digital data processing is carried out using software specifically made for this purpose. Meanwhile, visual analysis and interpretation are used if digital data processing cannot be carried out and does not function properly. Land Use Classification of Landsat Images is interpreted to produce land cover maps for 2008, 2013, and 2018. After obtaining the land cover map, an accuracy test was conducted in the land cover classification results.

Each land cover and land use class are sampled for accuracy testing. The land cover classification results in an accuracy test using the confusion matrix table. The Kappa coefficient is also calculated because it is not overestimated in determining the accuracy value. The accuracy test uses very high-resolution images in the form of google earth and bing maps.

The method used for land change prediction analysis is Markov Chain with projections to 2028 Idrisi Selva 17.2 software. In this stage, projections are carried out by assuming that changes that will occur in the future have patterns and possibilities similar to the patterns of changes that occur over a period used by using software that can assist in managing satellite imagery for land use change analysis. Validation will be carried out from the land use modeling results, namely, comparing the land use data from the modeling with the data from the interpretation of the validation test images measured by the Kappa Index of Agreement (kappa value).

2.2.4. Erosion And Sediment Analysis

Erosion and sediment analysis were estimated using the Modified Universal Soil Loss Equation (MUSLE). MUSLE uses runoff quantities to simulate erosion and sedimentation. Based on the hydrological analysis, the predictions of runoff volume and runoff peak rates are obtained then used to analyze the energy of erosive runoff. Substitution of these parameters provides the following advantages: the accuracy of the model's prediction is increased, the delivery ratio is no longer needed, and a single rainfall forecast that produces sediment can be calculated.

Digital map is prepared and first converted to format according to ArcSWAT 2012 requirements (change shapefile to raster). Suppose the data is in the correct format. In that case, we can start running ArcSWAT by performing the following steps: Automatic Watershed Delineation, HRU Analysis, Write Input Tables, Edit SWAT Input, SWAT Simulation.

Calibration using SWAT-CUP software with SUFI-2 program. The output of the 2012 ArcSWAT model is then calibrated and validated. Calibration and validation have the aim that the simulation results resemble the real situation in the field. Calibration and validation are done by comparing the simulation results with the monthly discharge from the observation results. Assessment of calibration and validation used helpful software, namely SWAT-CUP with the SUFI-2 program. The calibration and validation assessment parameters are P-factor, r-factor, NS, and R2.

3. Results and Discussion

3.1. Hydrological Analysis

Consistency Test

Consistency test was carried out with two methods, the double mass curve method for rainfall data at the rain station post.

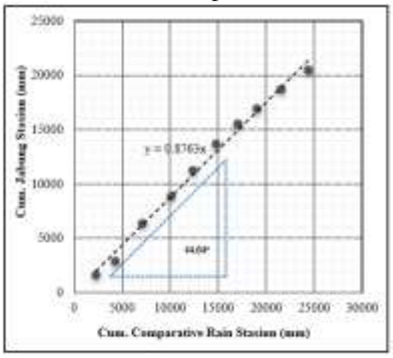

Figure 1. Double Mass Curve of Jabung Rain Station

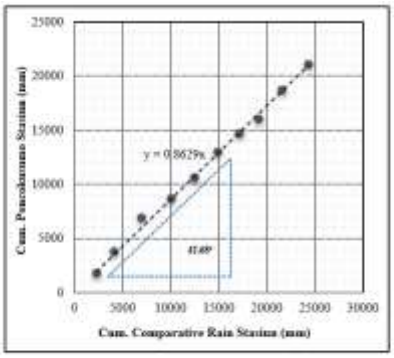

Figure 2. Double Mass Curve of Pocokusumo Rain Station

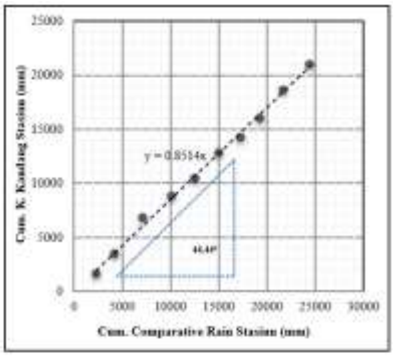

Figure 3. Double Mass Curve of Kedung Kandang Rain Station

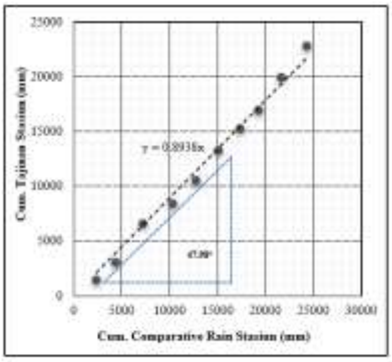

Figure 4 Double Mass Curve of Tajinan Rain Station

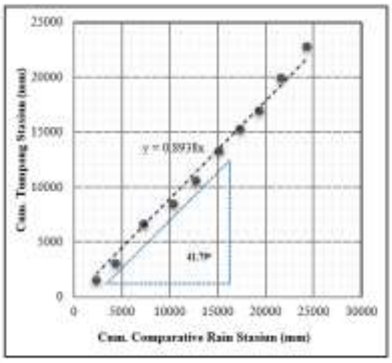

Figure 5. Double Mass Curve of Tumpang Rain Station

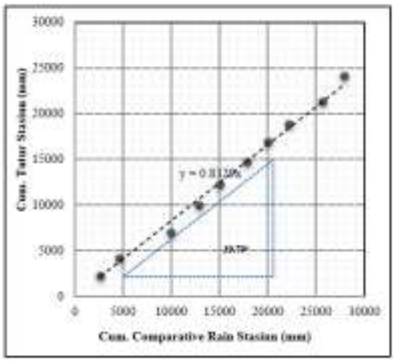

Figure 6. Double Mass Curve of Tutur Rain Station

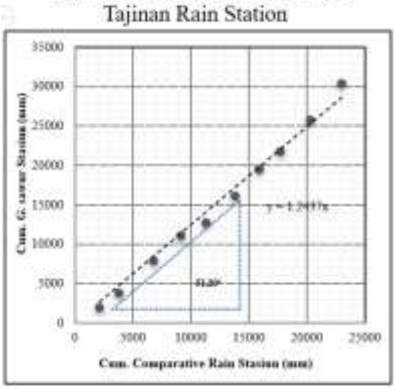

Figure 7. Double Mass Curve of Gunung Sawur Rain Station

The results of this test indicate that the selected data can be used for further hydrological testing and analysis. Based on Figures 1 to 7 of the double mass curve at each rain station above, it is known that there is a strong relationship between the x and y variables, with the coefficient of determination between 0.9 < R2 < 1. And it can be concluded that there were no deviations in the data from each station, so there was no correction on the rain data and the data was considered consistent.

Homogeneity Test

This study tested the annual rainfall data for rain stations for the absence of trends by the Spearman Method using a 2-sided T-Test. The recapitulation of test results is presented as follows.

Table 1. Recapitulation of No Trend Test Results

No.	Post Name	α	Tc Value (T Test Table)	Coefficient Distribution Number	Information
1	Jabung	5%	1.86	0.76	t<tc, no tren
2	Poncokusumo	5%	1.86	-1.19	t<tc, no tren
3	Kedung Kandang	5%	1.86	0.42	t<tc, no tren
4	Tajinan	5%	1.86	0.42	t<tc, no tren
5	Tumpang	5%	1.86	-0.56	t<tc, no tren
6	Tutur	5%	1.86	0.36	t<tc, no tren
7	Gunung Sawur	5%	1.86	0.92	t<tc, no tren

Based on Table 1, it can be seen that the overall data does not show a trend by showing $t_{calculate}<t_{table}$ at 5% confidence level. Thus, these data can be analyzed further.

Table 2. Recapitulation of Variance Stability Test Results (F Test)

No.	Post Name	α	Fc Value (F Test Table)	Coefficient Distribution Number	Information
1	Jabung	5%	5.192	0.19	$F < F_c$, stable
2	Poncokusumo	5%	5.192	0.40	F < Fc , stable
3	Kedung Kandang	5%	5.192	0.20	F < Fc , stable
4	Tajinan	5%	5.192	1.37	F < Fc , stable
5	Tumpang	5%	5.192	0.78	F < Fc , stable
6	Tutur	5%	5.192	1.89	F < Fc , stable
7	Gunung Sawur	5%	5.192	0.88	F < Fc , stable

Table 3. Recapitulation of Average Stability Test Results (t Test) Annual Period

No.	Post Name	α	Tc Value (T Test Table)	Coefficient Distribution Number	Information
1	Jabung	5%	1.943	0.95	T < tc , stable
2	Poncokusumo	5%	1.943	0.40	T < tc , stable
3	Kedung Kandang	5%	1.943	0.10	T < tc , stable
4	Tajinan	5%	1.943	3.37	T < tc , stable
5	Tumpang	5%	1.943	0.78	T < tc , stable
6	Tutur	5%	1.943	4.89	T < tc , stable
7	Gunung Sawur	5%	1.943	0.88	T < tc , stable

From Table 2 and Table 3 above, it can be seen that the value of F calculates < the value of F table and value of t calculate < value of t table, so it can be concluded that the rainfall data for the seven rain stations used has a stable variance and average.

The persistence test is an independent test for each value in the periodic series. First, the Spearman Method must calculate the number of serial correlation coefficients. The calculation of the persistence test with the T-test is carried out. The recapitulation of test results is presented as follows.

Table 4. Recapitulation of Persistence Test Results

No.	**Post Name**	**α**	**Tc Value (T Test Table)**	**Coefficient Distribution Number**	**Information**
1	Jabung	5%	1.860	2.00	T < tc , random
2	Poncokusumo	5%	1.860	8.00	T < tc , random
3	Kedung Kandang	5%	1.860	1.00	T < tc , random
4	Tajinan	5%	1.860	5.00	T < tc , random
5	Tumpang	5%	1.860	2.00	T < tc , random
6	Tutur	5%	1.860	3.00	T < tc , random
7	Gunung Sawur	5%	1.860	0.00	T < tc , random

Based on Table 4, it can be seen that almost all of the data are random by showing $t_{calculate} < t_{table}$ at 5% confidence level. Thus, these data can be analyzed further.

3.2 Regional Average Rainfall Analysis

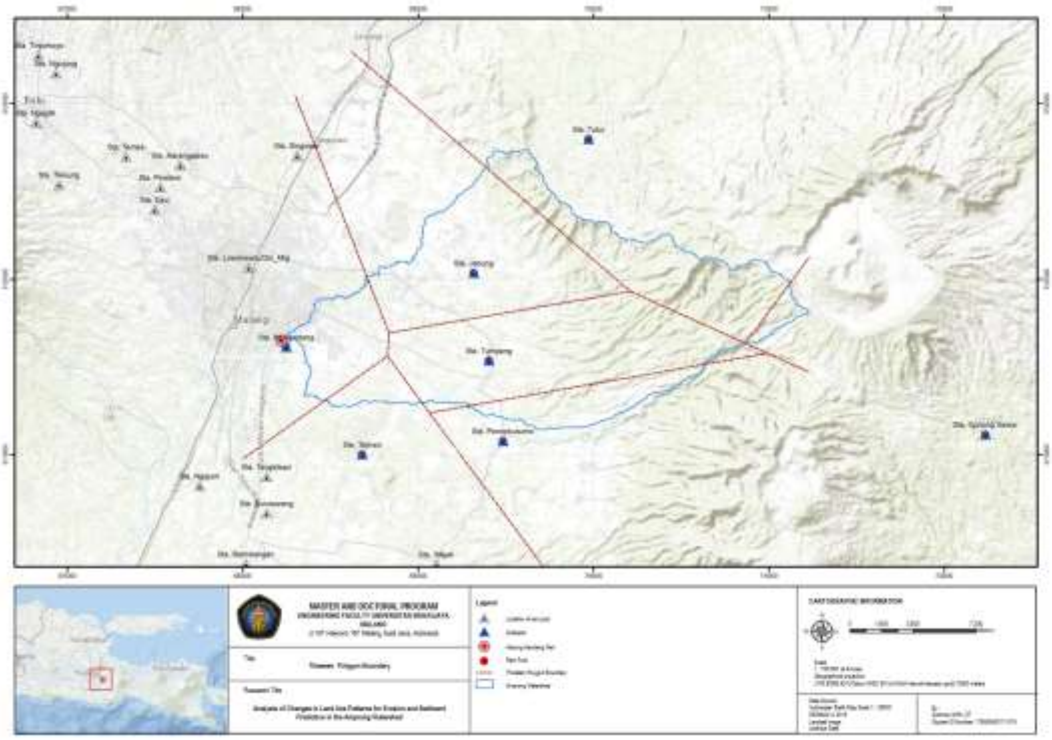

Figure 8. Map of the Influence Area of the Amprong Sub-watershed Rain Station Post using the Thiessen Polygon Method

Table 5. Amprong Sub-Watershed Thiessen Coefficient

Name	Area (km^2)	Persentase
Sta. Jabung	70.570	27.9%
Sta. Poncokusumo	23.018	9.1%
Sta. Kedung Kandang	23.270	9.2%
Sta. Tajinan	5.818	2.3%
Sta. Tumpang	80.435	31.8%
Sta. Tutur	48.564	19.2%
Sta. Gunung Suwur	1.265	0.5%
Total	252.94	100%

3.3. Land use change analysis

From the results of the classification of Landsat 7 ETM+ imagery in 2008, Landsat 8 OLI TIRS imagery in 2013, and Landsat 8 OLI TIRS imagery in 2018 in the Amprong watershed with an area of 252.94 km^2 in the period 2008 to 2018 (Table 5), as well as the results of observations conducted in the field for land use In the Amprong watershed, land use in the Amprong watershed is divided into six classes, namely garden forest, open land, settlements, rice fields, and a mixture of shrubs (Figure 8). The results of the interpretation of land use then conducted the accuracy test from the classification results obtained by comparing the interpretation of field use with high-resolution image data for each year of the determined land cover. From the six classes of land use interpretation results, 60 random points were checked with the number based on the percentage of each land cover each year to prove the accuracy of the interpretation of the map made. This accuracy test aims to determine the percentage of data confidence from Landsat image interpretation based on the confusion matrix table. The confusion matrix table can be presented as follows:

Table 6. Confusion matrix of sample point for each land-use class in 2008

Landsat Image Interpretation 2008	Code	Google Image 2008						Grand Total
		FRST	AGRL	PAST	URBN	RICE	RNGB	
	Forest Mixed (FRST)	**15**	3					**18**
	Agricultural Land Generic (AGRL)		**12**				1	**13**
	Open Field/Pasture (PAST)			**4**				**4**
	Urban (URBN)		1		**4**			**5**
	Rice (RICE)		3		1	**11**		**15**
	Range Brush (RNGB)						**5**	**5**
	Grand Total	**15**	**19**	**4**	**5**	**11**	**6**	**60**

Table 7. Confusion matrix of sample point for each land use class in 2013

Landsat Image Interpretation 2013	Code	Google Image 2013						Grand Total
		FRST	AGRL	PAST	URBN	RICE	RNGB	
	Forest Mixed (FRST)	14		1				**15**
	Agricultural Land Generic (AGRL)		11		1	1	2	**15**
	Open Field/Pasture (PAST)		2	1				**3**
	Urban (URBN)		1		5			**6**
	Rice (RICE)		1			14	2	**17**
	Range Brush (RNGB)						4	**4**
	Grand Total	**14**	**15**	**2**	**6**	**15**	**8**	**60**

Table 8. Confusion matrix of sample point for each land use class in 2018

Landsat Image Interpetation 2018	Code	Google Image 2018						Grand Total
		FRST	AGRL	PAST	URBN	RICE	RNGB	
	Forest Mixed (FRST)	14						**14**
	Agricultural Land Generic (AGRL)		11	1	1		2	**15**
	Open Field/Pasture (PAST)						1	**1**
	Urban (URBN)				8			**8**
	Rice (RICE)		2			11		**13**
	Range Brush (RNGB)		1				8	**9**
	Grand Total	**14**	**14**	**1**	**9**	**11**	**11**	**60**

Image classification accuracy test results (*Supervised Classification*) from the Amprong watershed confusion matrix table using ENVI 5.1 software were evaluated for accuracy with overall accuracy results for land cover interpretation in 2008 amounted to 85.00% in 2013 equal to 81.67%, and in 2018 amounted to 86.67%, while by the kappa accuracy for 2008 amounted to 80.86%, in 2013 equivalent to 76.73%, and in 2018 amounted to 83.33%, so it can be concluded that the interpretation of land cover with basic data of Landsat imagery is overall acceptable and can be used for the analysis of land cover projections in 2028 (Table 6-7).

Land use patterns experiencing dynamic changes from the analysis of land cover change dynamics in the Amprong watershed from 2008, 2013, and 2018. The trend of forest land cover change from 2008, 2013, and 2018 continues to decline with an average of 11.69% of the total land cover in 2008. This is inversely proportional to settlement cover, which is always increasing, as the average increase is 9.29% (Table 9 – 10).

Table 9. Land cover change matrix for 2008 – 2013

Land Cover	Year	2013						Grand Total
		Forest Mixed	Agricultural Land Generic	Pasture	Urban	Rice	Range Brush	
Forest Mixed	**2008**	6239.61	453.20	92.52	7.14	214.26	570.03	7576.76
Agricultural Land Generic		1.35	4041.55	16.18	355.11	1058.25	31.91	5504.35
Open Field/Pasture		114.22	283.39	1055.97	13.28	287.35	28.36	1782.57
Urban					2110.37			2110.37
Rice			1205.59	9.55		4842.55		6057.69
Range Brush		44.15	468.90	0.18	13.11	789.51	946.70	2262.56
Grand Total		6399.33	6452.63	1174.39	2499.02	7191.93	1577.00	25294.30

Table 10. Land cover change matrix for 2013 – 2018

Land Cover	Year	2018						Grand Total
		Forest Mixed	Agricultural Land Generic	Pasture	Urban	Rice	Range Brush	
Forest Mixed	**2013**	5311.77	571.09	142.75	1.42		372.30	6399.33
Agricultural Land Generic		436.88	3904.07	34.77	112.04	570.81	1394.06	6452.63
Open Field/Pasture		47.12	384.42	734.89	6.54	1.13	0.28	1174.39
Urban					2499.02			2499.02
Rice			1576.47	369.04	339.10	4826.49	80.83	7191.93
Range Brush		68.22	413.43	7.95	75.77	219.55	792.08	1577.00
Grand Total		5897.58	6515.21	512.75	3360.05	5424.18	3584.54	25294.30

3.4. Analysis of Land Cover Change Projections

Land cover projections were carried out using the Markov Chain Cellular Automata method. Land use in 2028 is obtained by comparing changes between 2008 and 2018. Model simulation was run with CA Markov. Projection analysis with 2008 and 2013 land use to predict the 2018 land use. This projection aims to map the 2018 predictions so that they can be validated with the actual 2018 land use maps that have been made previously. The validation results will bring up the kappa value obtained through the *tools Validate* on the idrisi selva. The validation value described in the kappa value has a maximum level of agreement between the number of rows and columns of 1,00. Kappa value > 0,81 indicates very good agreement/suitability, Kappa value = 0,61–0.80 good agreement/suitability, Kappa value 0.41-0.60 indicates sufficient agreement/suitability, Kappa value 0,21 -0.40 indicates a weak agreement/suitability, and a Kappa value <0,20 indicates a very weak agreement/suitability (Landis and Kock, 1977). The validation results between the actual 2018 land use and land use prediction of K standard value show the suitability/agreement of distribution and area of 85.85%. This condition indicates that our projections are acceptable (Figure 9).

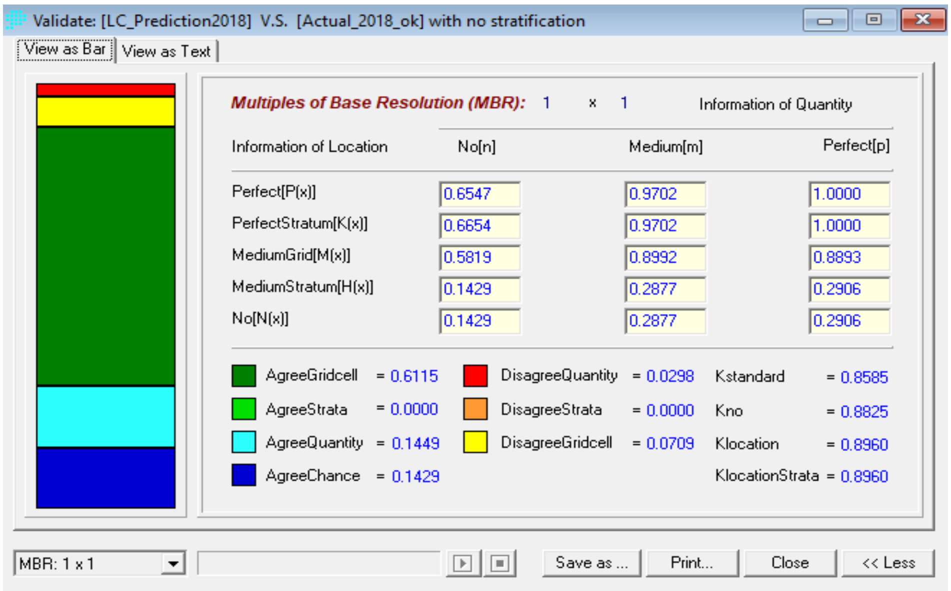

Figure 9. The results of the 2018 prediction land cover validation with the actual land cover from the image interpretation result

Land use in 2008 and 2018 was used to project land use in 2028. Changes in forest land cover decreased by 21.40%, gardens decreased by 4.33%, open land decreased by 42.11%, settlements increased by 46.47%, rice fields increased by 0.60%. Shrubs increased by 4.63% (Table 11) (Figure 10).

Table 11. Land cover change matrix for 2018 – 2028

Tutupan Lahan	Year	2028						Grand Total
		Forest Mixed	Agricultural Land Generic	Pasture	Urban	Rice	Range Brush	
Forest Mixed	2018	4833.78	75.91	27.40	0.71	0.32	959.45	5897.58
Agricultural Land Generic		1.72	5055.92	161.42	381.60	386.49	528.06	6515.21
Open Field/Pasture		8.02	69.54	424.53	2.09	1.98	6.59	512.75
Urban					3360.05			3360.05
Rice			221.03	120.21	350.08	4720.62	12.24	5424.18
Range Brush		121.40	334.95		19.11	246.24	2862.84	3584.54
Grand Total		4964.92	5757.36	733.55	4113.63	5355.66	4369.18	25294.30

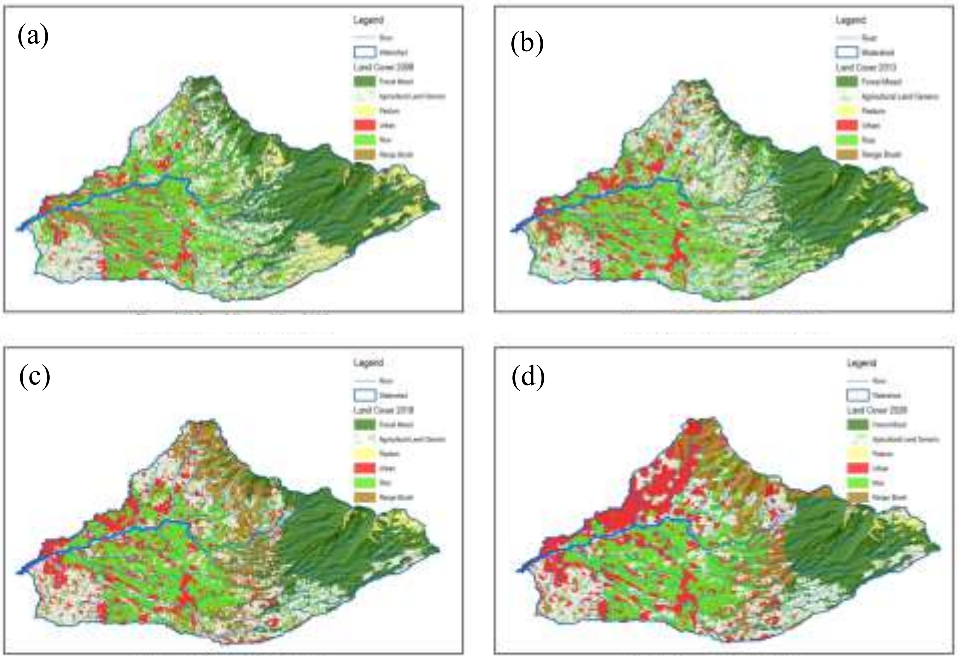

Figure 10. Land cover 2018 (a), 2013 (b), 2018 (c), 2028 (d)

3.4. Erosion And Sediment Analysis

HRU analysis process is carried out automatically by the SWAT program to produce the HRU (Hydrologic Response Unit). Watershed delineation in the HRU analysis process is based on map overlays, namely DEM maps, soil maps, and land cover maps. The main river network is formed based on the watershed delineation process results. The watershed boundary with a total 252.94 km^2 consists of 37 sub basins/subwatersheds. Formation of HRUs using Threshold by percentage, where each threshold percentage is 0% with 37 sub-watersheds formed. The HRUs generated from the analysis differ between land cover data in 2018, as many as 1254 HRU, and data with land cover in 2028 as many as 1073 HRU (Figure 11).

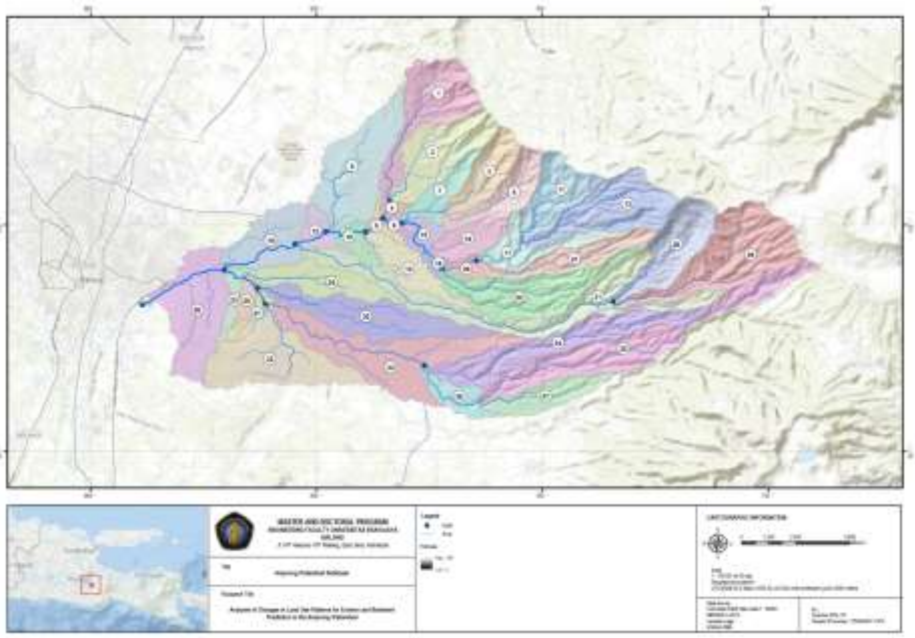

Figure 11. Amprong watershed subbasin

The results of hydrological modelling with land cover in 2018 in the Amprong watershed show that the average erosion of the Amprong watershed is 81.44 tons/ha/year with an average erosion value of 60.04 tons/ha/year (Figure 10). Based on the subbasin scale, the highest sedimentation occurred in subbasin number 11 amounted to157.67 tons/ha/year with an erosion value of 105.85 tons/ha/year, while the lowest sedimentation occurred in subbasin number 4 amounted to 31.12 tons/ha/year with the lowest erosion value of 24.95 tons/ha/year. Meanwhile, based on the HRU (Hydrology Response Unit) scale, the highest sedimentation occurred at HRU number 000110019 amounted to 1134.59 tons/ha/year, the largest erosion value equal to 777.22 tons/ha/year at HRU Number 000290010, while the lowest sedimentation was at HRU number 00170006 amounted to 0.46 tons/ha/ year with the lowest erosion value equal to 0.40 tons/ha/year at the same HRU number. Surface runoff from modelling result with land cover in 2018 an average of 772.78 mm/year. The total sediment in Amprong amounted to 1.021.237,49 tons/ha/year, and the erosion was equal to 752.973,95 tons/ha/year (Figure 12).

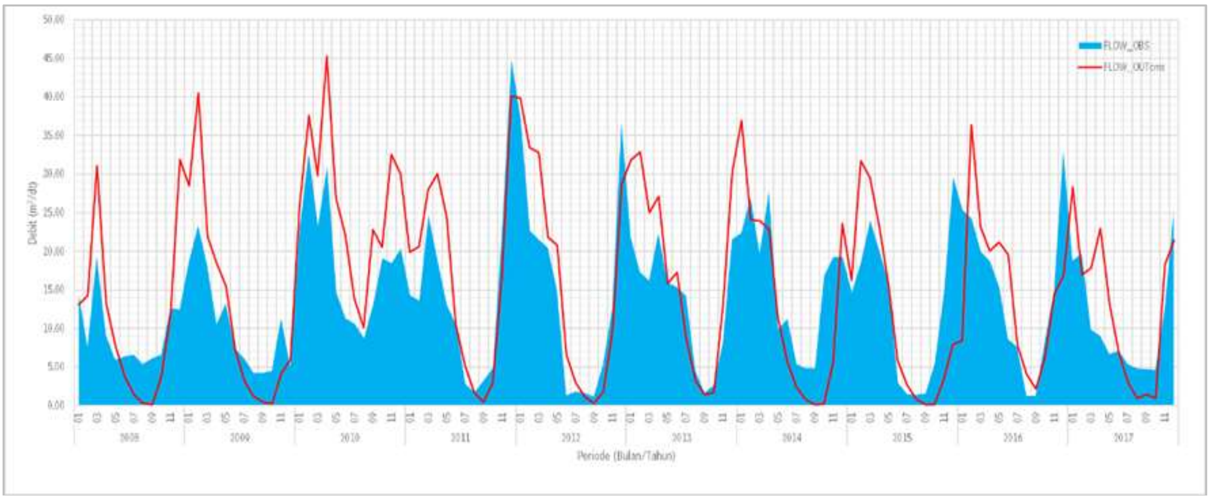

Figure 12. Comparison of simulation and observation discharge fluctuations in 2018

Discharge Data Calibration and Validation

Calibration and validation play a significant role in this study. With this process, the simulation results of the watershed model are expected to be close to the actual conditions. In the SWAT simulation process, there are many parameters used, these parameters will help in the calibration process. In this study, 8 parameters were used, among others: CN2 (SCS Curve Number), ALPHA_BF (Alpha factor for surface runoff), GW_DELAY (deceleration of groundwater flow), GWQMN (water threshold depth in shallow aquifers), GW_REVAP (Groundwater Revap coefficient) , AT_TTIME (lateral flow travel time), ESCO (soil evaporation replacement factor), USLE_P (land management factor). Monthly discharge data from observation discharge data taken from the Amprong Dam in 2010 - 2013 are also used as calibration input. The results of the data calibration process using SUFI2.SWAT-CUP can be seen in the Calibration outputs. The 95ppu.sf2 file contains the calibration process results in graphical form, as shown in Figure 13. The area of the green graph (95PPU) shows the discharge from the SUFI2.SWAT-CUP simulation result. The red line shows the best simulation results (best estimation), and the blue line indicates the observation result data at the Amprong Dam. The model calibration results obtained the coefficient of determination (R2) amounted to 0.84, and the value of Sutcliffe Model Efficiency (NS) was equal to 0.54. The number of input parameters is eight parameters. Later, this new parameter will be used as input in the validation process (Figure 13).

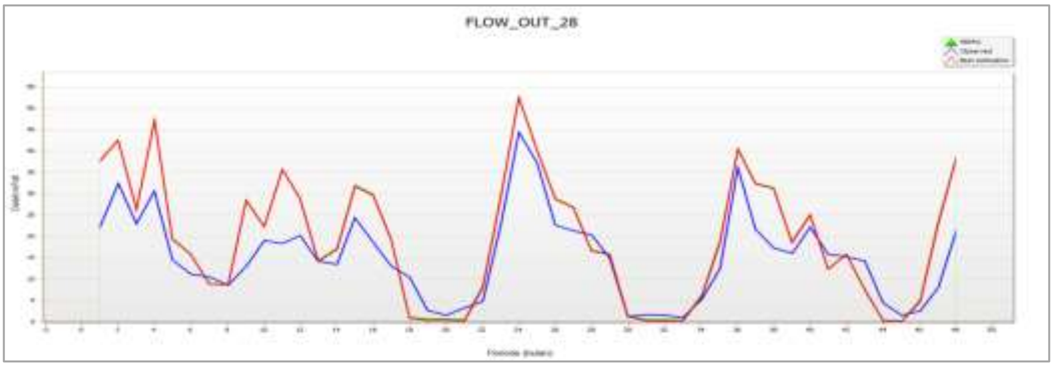

Figure 13. Graph of calibration results for Amprong Watershed River discharge data (*flowout 28*)

Validation was carried out using monthly discharge data for the 2014 – 2017 Amprong Watershed. The validation process shows unsatisfactory results, the value of the determination coefficient (R2) was 0.86, and the Nash-Sutcliffe Efficiency Model (NSE) simulation result was also unsatisfactory at -0.18. The results of this new parameter are used for the hydrological modeling process with land cover in 2028 (Figure 14). The hydrological system is sometimes affected by extraordinary (extreme) events, such as heavy rains, floods, and droughts. These conditions can happen because of the extraordinary extreme river discharge as seen far above the average discharge of the previous year.

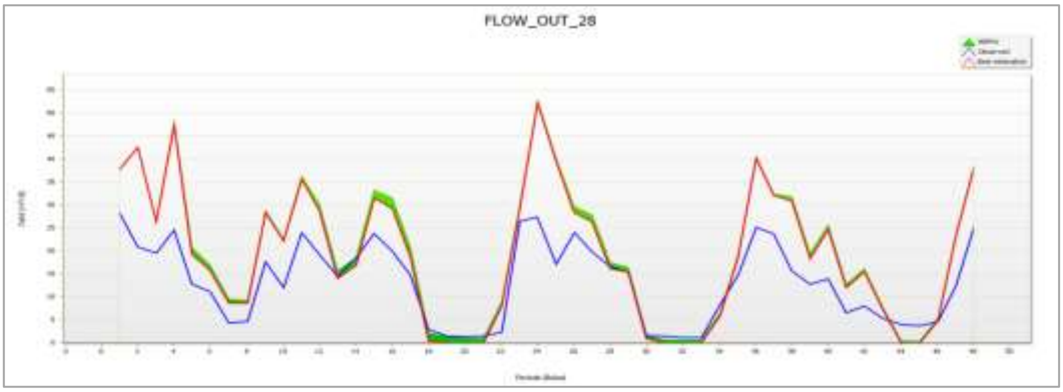

Figure 14. Graph of the validation results of the Amprong watershed River discharge data (*flowout 28*)

For hydrological modeling with land cover in 2028, the average erosion of the Amprong watershed amounted to 175.83 tons/ha/year with an average erosion value equal to 99.68 tons/ha/year. Based on the subbasin scale, the highest sedimentation occurred in subbasin number 26 amounted to 317.85 tons/ha/year with an erosion value of 185.46 tons/ha/year, while the lowest sedimentation occurred in subbasin number 6 amounted to 80.68 tons/ha/year with the lowest erosion value of 53.55 tons/ha/year in subbasin number 10. Meanwhile, based on the HRU (Hydrology Response Unit) scale, the highest sedimentation occurred at HRU number 000260008 at 2537.09 tons/ha/year, the highest erosion value was 1180.1694 tons/ha/year at the same HRU while the lowest sedimentation was at HRU number 000310008 at 1.96 tons/ha/ year with the lowest erosion value of 1.66 tons/ha/year at HRU number 000170004. Surface runoff from modeling results with land cover in 2028 an average of 907.28 mm/year, and for the total sediment in the Amprong watershed amounted to 1.886.689,64 tons/ha/year and the erosion equal to 1.069.631,09 tons/ha/year (Figure 15).

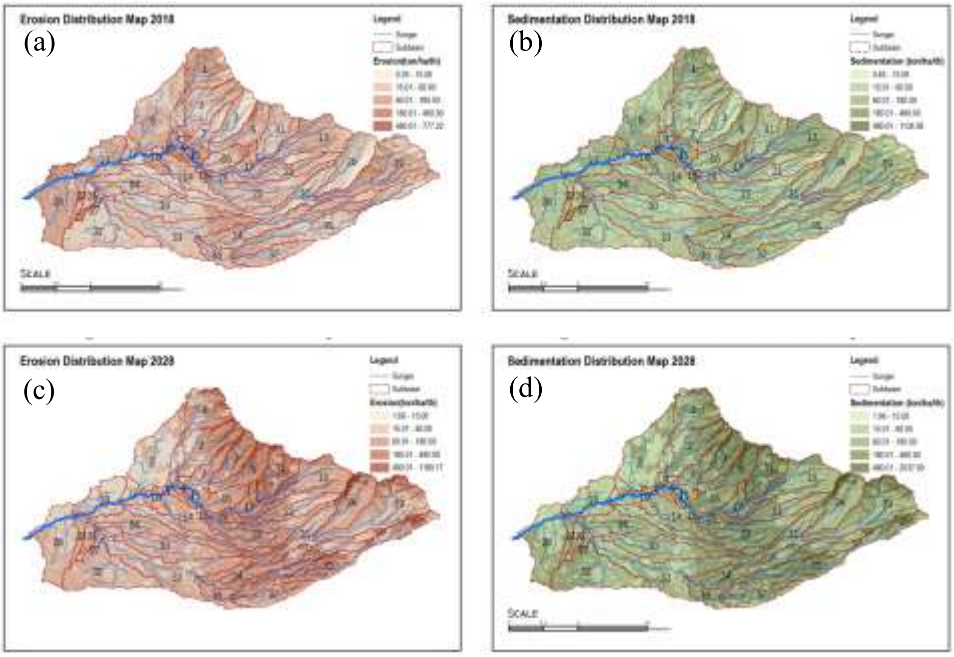

Figure 15. Errosion Distribution Map 2018 (a), 2013 (b), 2018 (c), 2028 (d)

3.5. Critical Land Analysis

In this study, the determination of critical land is carried out using the scoring method for land criticality determinant parameter. This scoring method refers to the Regulation of the Director General of Watershed Management and Social Forestry Number: P. 4/v-set/2013 on the Technical Guidelines for the Compilation of Spatial Data on Critical Lands. The parameters used are land slope conditions, vegetation cover (land coverage), erosion, and management. These parameters will be weighted and assessed for each. After that, an overlapping process is carried out to get the total weight value.

1) Land Coverage Map Making

This study's land cover maps were made digitally by analyzing Landsat 8 image data with image processing software. They used the NDVI (Normalized Difference Vegetation Index) process to determine the land coverage. NDVI calculates the greenness of leaves by using the ratio of the near infrared band (NIR) and the red band (Red). The NDVI formula is:

$$NDVI = \frac{(NIR - red)}{(NIR + red)}$$

The data used in this NDVI process is Landsat 8 imagery with band 4 (red) and band 5 (NIR). Later, a map of land coverage is obtained, classified into five classes. The calculation of density class interval is based on the following formula:

$$KL = \frac{xt - xr}{k}$$

Where KL is interval class, xt is the highest value, xr is the lowest value, and k is the desired number of classes. From the analysis results, it can be seen that the land coverage in the Amprong watershed is in very good condition 20.00%, good 24.85%, moderate 31.48%, bad 19.42%, and very bad 4.25%.

2) Land Slope

Land slope data was analyzed based on DEM data downloaded from the BIG website in the form of raster data. The land slope data in this study was obtained from the running results of Arcswat on the HRU file that had been carried out. With the division of slope classes into 5 classes, namely 0%-8% (flat), 8%-15% (sloping), 15%-25% (slightly steep), 25%-40% (steep), and >40% (very steep). From the analysis results, it can be seen that the slope of the land in the Amprong watershed is 27.61% flat, 20.21% sloping, 2.97% slightly step, 15.30% steep, and 23.81% very steep.

3) Erosion Hazard Level
The Erosion Hazard Level/Tingkat Bahaya Erosi (TBE) is calculated by comparing the level of erosion in a land unit (land unit) and the effective soil depth (solum) in that land unit. The erosion hazard level class is divided into five classes based on Permenhut No. P32/Menhut-II/2009. From the results of the analysis, it can be seen that the Hazard Level of Land Erosion in the Amprong Watershed with Class I (<15 tons/ha/year) equal to 14.87%, Class II (15-60 tons/ha/year) amounted to 36.90%, Class III (60- 180 tons/ha/year) 30.79%, Class IV (180-480 tons/ha/year) 13.27%, and Class III (>480 tons/ha/year) 4.17%.

4) Land Management
In relation to the preparation of critical land spatial data, these criteria need to be spatialized using or based on certain mapping units. The mapping unit used, referring to the mapping unit for productivity criteria, is the land system mapping unit. Management criteria in determining critical land are divided into three classes. The map shows that land management in the Amprong watershed has a good class of 44.84%, a medium class of 23.67%, and a bad class of 31.48%.

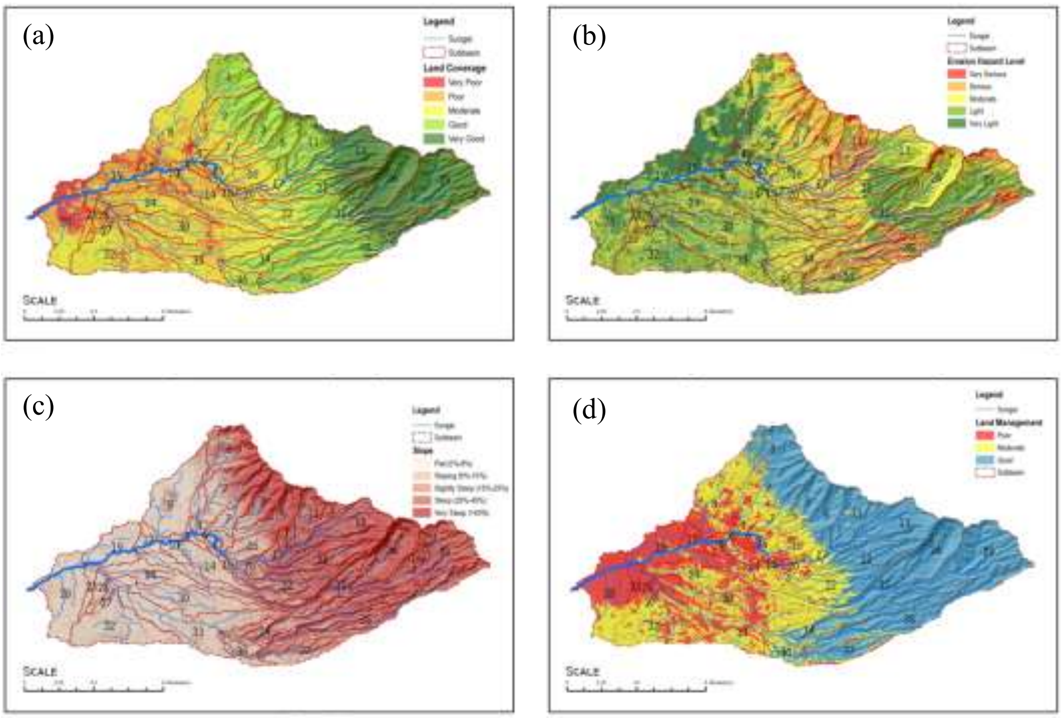

Figure 16. Land coverage map (a), Erosion Hazard Level Map (b), Map of Land Slope (c), Land Management Map (d)

From the results of the overlay parameters that determine the land criticality, it can be seen that in the Amprong watershed. From the total watershed area of 25294.74 ha, most of them are categorized as critical land, namely amounted to 11.86%, slightly critical land amounted to 48.17%, potentially critical land equal to 38.25% non-critical land equal to 1.72% (Figure 16 - 17).

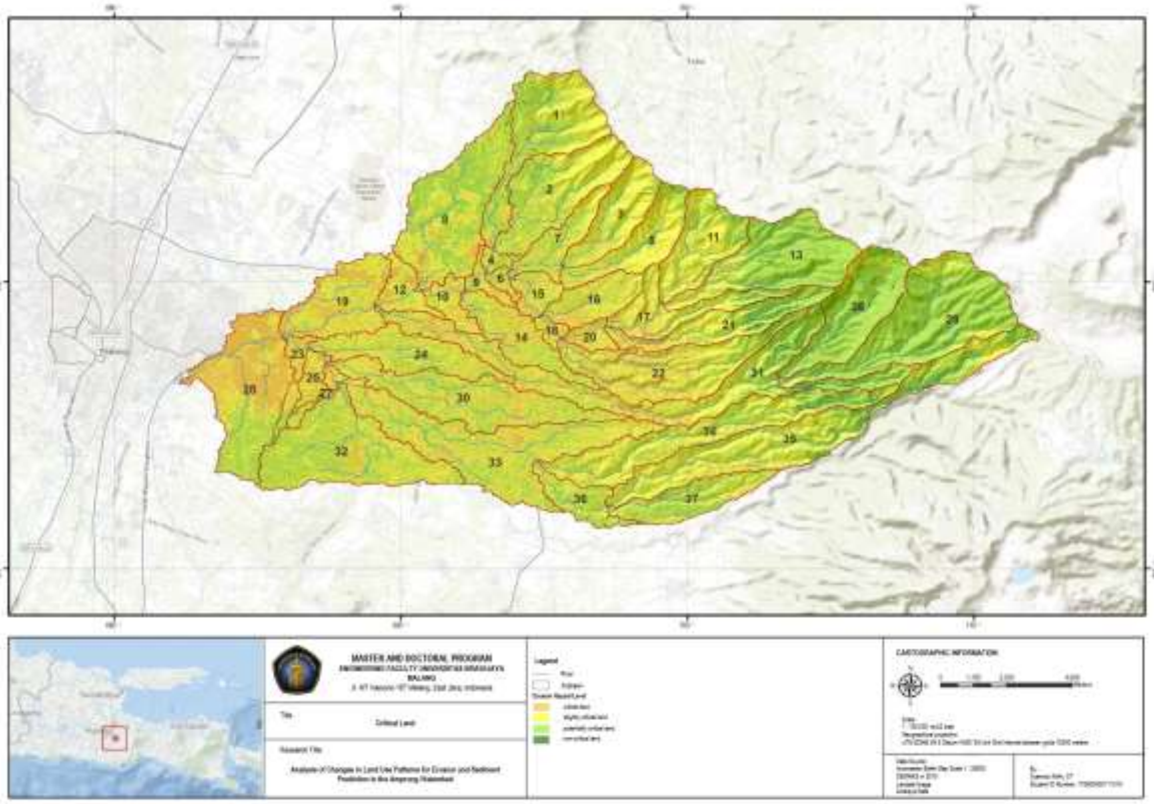

Figure 17. Map of Land Criticality for Protected Areas in the Amprong Watershed

3.6. Directions for Watershed Land Conservation

Vegetative Land Conservation

As for the types of vegetative land conservation are as follows:

1. Alley Cropping
2. Reforestation
3. Agroforestry
4. Relay cropping
5. Planting the cover crops as green manure
6. Living fence
7. Mixed garden
8. Strip cropping
   Strip cropping is the planting of two or more types of plants in alternating strips between the main crop and the ground cover crop. This system is applied to land with slopes of 15-40%.
   The effectiveness of vegetative conservation with strip cropping conservation methods in the Amprong watershed can be seen to be able to reduce sediment in the watershed by 8.61% from 1.069.631,01 tons/ha/year (403.634,29 m^3/year) to 977.506,68 tons/ha/year (368.870,44 m^3/year)
9. Riparian Buffer Strip (Filter Strip)
   Riparian buffer/filter strip functions to preserve the function of the river by holding back or capturing eroded soil (mud) as well as nutrients and chemicals including pesticides that are carried away from the land on the left and right of the river so that they do not enter the river.
   The effectiveness of vegetative conservation with the Filter Strip conservation method in the Amprong watershed is not able to reduce sediment in the watershed but can reduce the sedimentation rate by 29% from 1,886,689.64 tons/ha/year to 1,334,937.30 tons/ha/year.
10. Mulch
11. Environmental Greening

Mechanical Land Conservation

This method is an effort to conserve soil by using soil management techniques and civil structure construction which are expected to reduce the rate of water erosion. The general methods used in this method among others:

1. *Contour tillage*
   The soil tillage parallel to the contour lines and form small ridges that slow down the flow of water and increase water infiltration.
   The effectiveness of mechanical conservation with the Contour tillage conservation method in the Amprong watershed. From the results of the SWAT model, it is known that it is able to reduce sediment in the watershed by 48.91% from 1.069.631,01 tons/ha/year (403.634,29 m^3/year) to 546.499,59 tons/ha/year (206.226,26 m^3/year)
2. *Terracing*
   It is the creation of terraces on sloping land to reduce the angle of the land so that erosion can be minimized. The effectiveness of mechanical conservation with the Terracing conservation method in the Amprong watershed. From the results of the SWAT model, it can be seen that it can reduce sediment in the watershed by 31.57% from 1.069.631,01 tons/ha/year (403.634,29 m^3/year) to 731.976,44 tons/ha/year (276.217,52m^3/year)
3. Guludan/Bedengan
4. Checkdam
   It is an activity to stem the flow of water through a ditch so that the eroded material can be retained and deposited. Mechanical conservation is recommended in locations with severe/heavy and very severe/heavy Erosion Hazard Levels (TBE).
   The effectiveness of mechanical conservation in the Amprong watershed can be determined by reducing sediment that comes out of the outlet of the Amprong watershed. The SWAT model results with potential sediment that can be accommodated from the twenty-eight planned check dams. Sediment outflow at the outlet of the Amprong watershed from the hydrological model (SWAT) was 1,069,630.87 tons/year or 403.634.29m^3/year. By building twenty-eight check dams at these locations, it is able to reduce sediment by 397,757.39 tons/year or 162.406,97m3/year (40.24%) of the total sediment in the Amprong watershed (Table 12 – 13)(Figure 18).

Table 12 Location of the Check Dam Placement

No. Check Dam	No. Subdas	Coordinate		No. Check Dam	No. Subdas	Coordinate	
		X	Y			X	Y
1	1	693160.28	9121312.30	15	16	695893.33	9118972.83
2	1	694246.35	9124583.93	16	21	697369.06	9118364.83
3	2	693302.98	9121176.02	17	21	699956.41	9118184.89
4	2	694178.03	9122413.08	18	21	701712.65	9118412.73
5	2	695012.98	9122132.23	19	22	695644.59	9117922.45
6	5	695747.53	9120459.05	20	22	697241.36	9117150.14
7	5	698367.93	9121213.79	21	22	696852.14	9116779.90
8	5	697358.41	9120621.74	22	29	703429.77	9116517.85
9	13	699315.37	9119160.82	23	29	707598.42	9117852.63
10	13	700925.99	9120432.42	24	35	697421.73	9112261.15
11	13	701332.92	9120377.82	25	35	699804.52	9113514.25
12	13	700953.20	9119969.61	26	36	694767.18	9113704.72
13	16	694995.10	9118869.50	27	36	696747.72	9112080.78
14	16	696709.74	9119485.46	28	36	695333.23	9112840.23

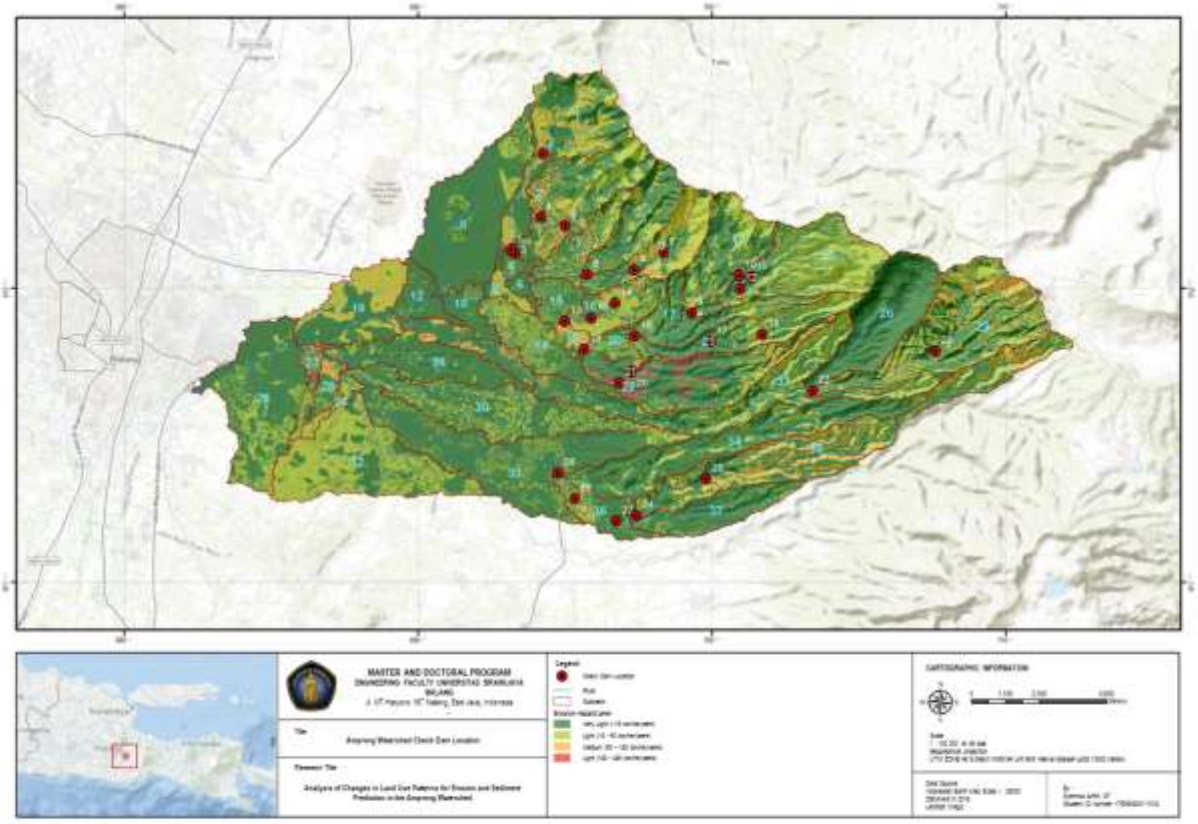

Figure 18. Map of the Location of Check Dam Placement in the Amprong Watershed

4. Conclusion

Based on the results of data analysis, modeling, and discussions that have been carried out, the following conclusions can be drawn:

The land cover classification results in 2008 to 2018 show a dynamic changing trend. The trend of changes in forest land cover from 2008, 2013, and 2018 continued to decline with an average of 11.69% of the total land cover in 2008. This result is different from the 2008 land cover, which has consistently increased, while the average increase is 9, 29%. From land cover change modeling for 2028, forest land cover changes decreased by 21.40%, gardens decreased by 4.33%, open land decreased by 42.11%, increased by 46.47%, rice fields increased by 0.60%, and shrubs increased 4.63%. The results of hydrological modeling with land cover in 2018 in the Amprong watershed, the value of surface runoff, total sediment, and erosion increased in 2028 in the Amprong watershed, the amount of surface runoff from the modeling results with land cover in 2028 an average of 907.28 mm/year, and for the total sediment in Amprong watershed increased by 85.75% to 1,886,689.64 tons/ha/year and erosion increased by 42.05% to 1,069,631.09 tons/ha/year. Non-critical land is equal to 15.66%. Critical potential land is 49.35%, slightly critical land is 29.33%. Critical land by 5.66%, and very critical by 0.01%. As a conservation recommendation in handling the Amprong watershed by applying vegetative and mechanical conservation. The results of the analysis and simulation of hydrological models using vegetative and mechanical methods are quite effective in reducing the impact caused by cover changes, namely the increase in sediment in the Amprong watershed.

Table 13 The effectiveness of the application of vegetative and mechanical conservation

Information	Average				Total Sedimen t	Total Erosion		Effectiveness
	Sediment (ton/ha/year)	Erosion (ton/ha/year)	Rain (mm/year)	Runnoff (mm/year)	(ton/ha/year)	(ton/ha/year)	m^3/year	
Condition in 2018	81.44	60.05	2246.94	772.78	1,021,237.49	752,973.95	284,141.11	-
Condition in 2028	175.83	99.69	2262.66	907.29	1,886,689.64	1,069,631.01	403,634.29	-
Conditions in 2028 with strip cropping conservation	130.85	91.10	2262.66	775.82	1,404,042.95	977,506.68	368,870.45	8.61%
Conditions in 2028 with terracing conservation	112.12	68.22	2262.66	738.04	1,203,026.41	731,976.44	276,217.53	31.57%
Conditions in 2028 with filter strip conservation	124.41	99.69	2262.66	907.29	1,334,937.30	1,069,631.01	403,634.29	0.00%
Conditions in 2028 with countouring conservation	50.93	68.62	2262.66	572.55	736,337.07	546,499.60	206,226.26	48.91%
Construction of check dam at 28 points						397,757.39	162,406.97	40.24%

References

[1] S. Utami, Soemarno, Surjono, and M. Bisri, "Disaster Risk and Adaptation of Settlement along the River Brantas in the Context of Sustainable Development, Malang, Indonesia," *Procedia Environ. Sci.*, vol. 20, pp. 602–611, 2014, doi: 10.1016/j.proenv.2014.03.073.

[2] A. C. Cindy Harifa, M. Sholichin, and T. B. Prayogo, "ANALISA PENGARUH PERUBAHAN PENUTUPAN LAHAN TERHADAP DEBIT SUNGAI SUB DAS METRO DENGAN MENGGUNAKAN PROGRAM ARCSWAT," *J. Tenik Pengair.*, vol. 008, no. 01, pp. 1–14, May 2017, doi: 10.21776/ub.jtp.2017.008.01.01.

[3] F. U. Hasanah, R. Wirosoedarmo, and B. Suharto, "Pemetaan Risiko Bencana Tanah Longsor di Sub Daerah Aliran Sungai Amprong," *J. Sumberd. Alam dan Lingkung.*, vol. 4, no. 3, pp. 10–17, Dec. 2017, doi: 10.21776/ub.jsal.2017.004.03.2.

[4] A. Riyadi, A. Rachmansyah, and B. Yanuwiadi, "Water Carrying Capacity Approach in Spatial Planning: Case Study at Malang Area," *J. Pembang. dan Alam Lestari*, vol. 9, no. 1, pp. 45–50, Feb. 2018, doi: 10.21776/ub.jpal.2018.009.01.08.

[5] L. M. Limantara, D. H. Harisuseno, and V. A. K. Dewi, "Modelling of rainfall intensity in a watershed: A case study in Amprong watershed, Kedungkandang, Malang, East Java of Indonesia," *J. Water L. Dev.*, vol. 38, no. 1, pp. 75–84, Sep. 2018, doi: 10.2478/jwld-2018-0044.

[6] A. K. Batar and T. Watanabe, "Landslide Susceptibility Mapping and Assessment Using Geospatial Platforms and Weights of Evidence (WoE) Method in the Indian Himalayan Region: Recent Developments, Gaps, and Future Directions," *ISPRS Int. J. Geo-Information*, vol. 10, no. 3, p. 114, Feb. 2021, doi: 10.3390/ijgi10030114.

[7] V. Mishra, P. Rai, and K. Mohan, "Prediction of land use changes based on land change modeler (LCM) using remote sensing: A case study of Muzaffarpur (Bihar), India," *J. Geogr. Inst. Jovan Cvijic, SASA*, vol. 64, no. 1, pp. 111–127, 2014, doi: 10.2298/IJGI1401111M.

[8] H. Haas, L. Kalin, and P. Srivastava, "Improved forest dynamics leads to better hydrological predictions in watershed modeling," *Sci. Total Environ.*, vol. 821, p. 153180, May 2022, doi: 10.1016/j.scitotenv.2022.153180.

[9] Y. Liu, G. Cui, and H. Li, "Optimization and Application of Snow Melting Modules in SWAT Model for the Alpine Regions of Northern China," *Water*, vol. 12, no. 3, p. 636, Feb. 2020, doi: 10.3390/w12030636.

[10] R. Haribowo, U. Andawayanti, and R. D. Lufira, "Effectivity test of an eco-friendly sediment trap model as a strategy to control erosion on agricultural land," *J. Water L. Dev.*, vol. 42, no. 1, pp. 76–82, 2019, doi: 10.2478/jwld-2019-0047.

[11] H. Yamashita *et al.*, "Toxicity test using medaka (Oryzias latipes) early fry and concentrated sample water as an index of aquatic habitat condition," *Environ. Sci. Pollut. Res.*, vol. 19, no. 7, pp. 2581–2594, Aug. 2012, doi: 10.1007/s11356-012-0906-0.

[12] M. Aslam and M. Albassam, "Presenting post hoc multiple comparison tests under neutrosophic statistics," *J. King Saud Univ. - Sci.*, vol. 32, no. 6, pp. 2728–2732, Sep. 2020, doi: 10.1016/j.jksus.2020.06.008.

[13] J. Lilienthal, R. Fried, and A. Schumann, "Homogeneity testing for skewed and cross-correlated data in regional flood frequency analysis," *J. Hydrol.*, vol. 556, pp. 557–571, Jan. 2018, doi: 10.1016/j.jhydrol.2017.10.056.

[14] C.-H. Liaw and Y.-C. Chiang, "Dimensionless Analysis for Designing Domestic Rainwater Harvesting Systems at the Regional Level in Northern Taiwan," *Water*, vol. 6, no. 12, pp. 3913–3933, Dec. 2014, doi: 10.3390/w6123913.